J. Iran. Chem. Soc., Vol. 7, No. 3, September 2010, pp. 554-563.

JOURNAL OF THE
Iranian
Chemical Society

Theoretical Study of Diels-Alder Reaction: Role of Substituent in Regioselectivity and Aromaticity

A. Mohajeri* and M. Shahamirian
Department of Chemistry, College of Sciences, Shiraz University, Shiraz 71454, Iran

(Received 10 March 2009, Accepted 12 July 2009)

A comparative study on the influence of the substituents on the Diels-Alder reaction was performed. The energy profiles for 11 sets of Diels-Alder reaction between monosubstituted derivatives of butadiene and ethylene have been studied and the structures of all transition states were located at B3LYP/6-31+G* level. Four pathways were independently investigated; the reaction between substituted ethylene and 1-substituted butadiene leading to *ortho* (***a*$_1$**) and *meta* (***a*$_2$**) adducts, and in the same manner, the reaction between substituted ethylene and 2-substituted butadiene yields *para* (***b*$_1$**) and *meta* (***b*$_2$**) adducts. Inspection of both the activation barriers and the reaction energies for 44 reactions revealed that the pathway ***b*$_1$** is both thermodynamically and kinetically more favorable in all types of Diels-Alder reactions; while the pathway ***a*$_1$** can be labeled only as kinetic pathway. The aromaticity of all 44 transition state structures was measured using *para* delocalization index to study the effect of aromaticity on the reaction path. The calculations suggest that in normal and neutral DA reactions there is a gain in aromatic stabilization of the transition state which reduces slightly the activation barrier of the kinetic pathway ***a*$_1$**.

Keywords: Diels-Alder reaction, Regioselectivity, Aromaticity, *para* delocalization index

INTRODUCTION

Among the methods in organic synthesis, the Diels-Alder (DA) reaction holds an important position which is strongly influenced by electronic and steric effects in both diene and dienophile [1]. Being the most favored one, the Diels-Alder reaction between butadiene and ethylene, has been studied at several levels of theory [2-11]. The DA reaction has proven to require opposite electronic arrangements at the diene/ dienophile pair for being reasonably fast. Generally speaking, this reaction is classified into three categories: (i) the normal electron demand DA reaction, which is activated by an energy gap decrease between HOMO of the electron-rich diene and the LUMO of the electron-poor dienophile; thus, a $HOMO_{diene}$-$LUMO_{dienophile}$ controlled (ii) the inverse electron demand DA reaction which is favored by electron-poor dienes with very low LUMOs and an electron-rich dienophile with a high HOMO, and therefore is $LUMO_{diene}$-$HOMO_{dienophile}$ controlled; (iii) the neutral DA reaction, in which both MO interactions are important. In most [4+2] cycloadditions, an electron-rich compound reacts with an electron-deficient partner to ensure a small HOMO-LUMO gap, which leads to a rapid reaction due to a good interaction of the frontier molecular orbitals (FMOs). This represents, at the same time, a synthetic limitation for the DA reaction in that reactants with similar electron demand usually react slowly.

The mechanism of the DA reaction has been the subject of the most heated and interesting controversies [12-16]. In particular, the DA reaction between butadiene and ethylene is often taken as the classic example of a pericyclic reaction.

*Corresponding author. E-mail: amohajeri@shirazu.ac.ir

Despite its apparent simplicity, the reaction mechanism nature is controversial and thus subject of numerous experimental and theoretical studies. The concerted nature of the mechanism and its stereospecificity have been established, although a stepwise mechanism can coexist involving the activation barrier merely a few kcal mol^{-1} higher [17,18]. A theoretical analysis of transition state (TS) stabilization in DA reactions of 23 substituted dienes revealed that substituents (de) stabilize transition states through four effects; steric, mesomeric, inductive and polarizability acting principally by favoring the electronic transfer between the two partners [19].

It is well-recognized that DA reaction takes place through an aromatic transition state. The aromaticity of pericyclic transition sates has been analyzed by Jiao and Schleyer on the basis of geometric, energetic and magnetic criteria [20]. Matito *et al*. analyzed the change in the aromaticity along the reaction path of DA reaction between ethylene and butadiene using several indices of aromaticity such as nucleus independent chemical shift (NICS), the Harmonic oscillator model of aromaticity (HOMA), *para* delocalization index (PDI), and aromatic fluctuation index (FLU) [21]. They found that structural-based indices such as HOMA and FLU fail to account for the aromaticity of the transition states while NICS and PDI correctly predict the aromatic character of species along the reaction path.

In the present work, detailed theoretical studies are reported on reactivity and regioselectivity of DA reaction in normal, inverse and neutral types. 1,3-Butadiene and ethylene were considered as standard diene and dienophile, respectively. Four substituents with different inductive and mesomeric effects (Schemes 1 and 2) have been selected and 44 DA reactions have been studied between substituted dienes and dienophiles. Our main goals are to investigate the role of substituent on 1) the potential energy surface and activation barrier of the reaction, 2) the thermodynamic or kinetic stability of the favored product and 3) the aromaticity of the transition states.

COMPUTATIONAL METHODS

Forty-four DA reactions in normal, inverse, and neutral types have been studied in order to provide a complete set of substituent effect on both diene and dienophile. The geometries of all reactants, transition states and products were optimized at density functional level using B3LYP method and 6-31+G* basis set. The frequency calculation was

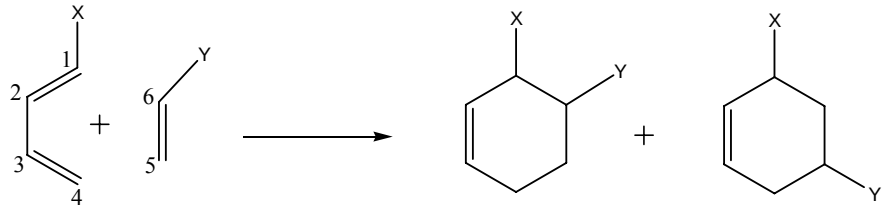

X, Y = Cl, CH_3, OCH_3, $COOCH_3$

Scheme 1

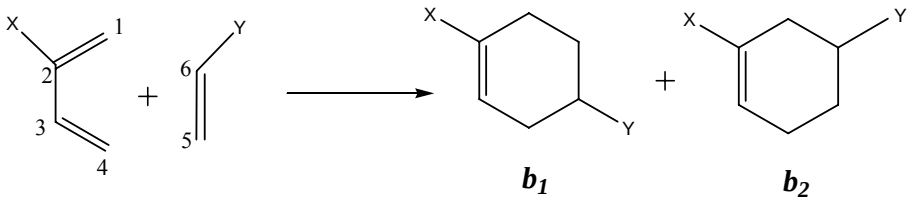

X, Y = Cl, CH_3, OCH_3, $COOCH_3$

Scheme 2

performed to verify the transition states with one imaginary frequency and the equilibrium structure with no imaginary frequencies. For each reaction the transition structure has been confirmed by intrinsic reaction coordinate (IRC) calculation for both forward and inverse directions [22,23]. All the calculations were carried out using Gaussian03 program [24]. The aromaticity of transition states were evaluated using *para* delocalization index (PDI) as the average of delocalization indices of *para* related atoms in a given six-membered ring [25],

$$\mathrm{PDI} = \frac{\delta(1,4) + \delta(2,5) + \delta(3,6)}{3}$$

where delocalization index, δ(A,B), is a quantitative measure of the number of electrons delocalized or shared between atomic basins A and B. The AIM2000 program has been employed to calculate the delocalization indices for atomic pairs [26].

In this paper, the notation **1, 2,…, 11** are used to label the DA reaction with different substituents on diene and dienophile as shown in Table 1. The transition states identified for four pathways presented in Schemes 1 and 2 are denoted as ***n*-a_1*TS***, ***n*-a_2*TS***, ***n*-b_1*TS*** and ***n*-b_2*TS*** where ***n*** is the reaction number.

RESULTS AND DISCUSSION

It is reasonable to expect that [4+2] cycloadditions proceed *via* an asymmetric transition state as indicated by application of the regioselectivity criterion. The DA reaction between two dissymmetrical reagents is non-synchronous where the π electrons of the two reactants form two new σ bonds in which one σ bond is formed more rapidly than the other.

In DA reactions, orientation effect is observed when both reagents are asymmetrically substituted. For a 1-substituted diene, a head-to-head (*ortho*) or a head-to-tail (*meta*) cycloaddition is possible (pathways $\boldsymbol{a_1}$ and $\boldsymbol{a_2}$ in Scheme 1). In this case, the *ortho* isomer is preferred (*ortho* rule). Reaction with a 2-substituted diene yields the head-to-tail (*para*) and the head-to-head (*meta*) cycloadducts (pathways $\boldsymbol{b_1}$ and $\boldsymbol{b_2}$ in Scheme 2), in which the *para* isomer is favored (*para* rule) [27].

In this research, our main purpose was to perform systematic calculations on the role of substituents in the thermodynamic or kinetic stability of the favored product. Four substituents with different inductive (F) and mesomeric (R) effects, (CH_3, OCH_3, Cl, and $COOCH_3$) are selected, and 44 DA reactions including the case with electron-donating substituent on diene and electron-withdrawing substituent on dienophile (normal type), the case involving electron-poor diene and electron-rich dineophile (inverse type) as well as neutral type in which both diene and dieneophile are electron-donating or electronwithdrawing substituents have been studied. In order to check the thermodynamic or kinetic stability of the favored product according to *ortho*- or *para*-rule, dienes are considered in both 1- and 2-substituted cases.

Substituent Effect on the Regioselectivity

Table 1 encompasses the total energies of products, transition states, the reaction Gibbs free energies as well as HOMO-LUMO gaps (HLG) found in DA reactions calculated at B3LYP/6-31+G* level. The geometries of all deines and dienophiles and the transition states are given in supplementary material. Butadienes are considered in their cis conformation which presents a more favorable geometry for cycloaddition and has a more efficient overlap with ethylene than the trans conformer.

The principal bond lengths which undergo significant changes along the reaction coordinate as well as the imaginary frequencies are embodied in Table 2 for transition state structures, using the nomenclature shown in Schemes 1 and 2. Both butadiene and ethylene geometries perturb upon the cycloaddition. The double bonds become longer by about 0.06 Å in both ethylene and butadiene. In the transition structures one sigma bond formation occurs faster than the other. In most TSs, the distances for the bonds to be formed are in the range of 2.0-2.4 Å for both C_4-C_5 and C_1-C_6. The structure of optimized transition states for the reaction 1 is shown in Fig. 1 as representative examples of normal DA reaction.

Natural population analysis allows the evaluation of charge transfer and its direction [28]. The calculated charge transfer (CT) at B3LYP/6-31+G* level are reported in Table 2. It is obvious that in normal type of DA charge transfer occurs from diene toward dienophile whereas in inverse type DA the direction of CT is reversed. In most cases the maximum CT occurs in the pathway $\boldsymbol{a_1}$. The results show that the increase of

Table 1. Energies for Products and Transition States and the Reaction Gibbs Free Energies as well as HLG in DA Reaction Between Substituted Ethylene and Butadiene

Reaction NO.	X	Y	Product	E_{prod} (Hartree)	E_{TS} (Hartree)	$\Delta G_{reaction}$ (kcal mol^{-1})	HLG (kcal mol^{-1})
1	CH_3	Cl	***a*** $_1$	-733.56955	-733.47031	-22.20	127.61
			a $_2$	-733.57115	-733.46888	-23.29	127.61
			b $_1$	-733.57699	-733.46858	-26.33	132.19
			b $_2$	-733.57527	-733.46823	-25.18	132.19
2	Cl	CH_3	***a*** $_1$	-733.56976	-733.46915	-22.61	123.54
			a $_2$	-733.57238	-733.46842	-24.70	123.54
			b $_1$	-733.57261	-733.46910	-25.28	121.99
			b $_2$	-733.57026	-733.46898	-23.48	121.99
3	OCH_3	Cl	***a*** $_1$	-808.77483	-808.67940	-18.73	116.56
			a $_2$	-808.77691	-808.67717	-20.14	116.56
			b $_1$	-808.78776	-808.67693	-25.23	127.48
			b $_2$	-808.78571	-808.67540	-23.90	127.48
4	Cl	OCH_3	***a*** $_1$	-808.77538	-808.67880	-20.50	105.97
			a $_2$	-808.77817	-808.67882	-22.18	105.97
			b $_1$	-808.77848	-808.67921	-22.77	104.42
			b $_2$	-808.77830	-808.67904	-22.59	104.42
5	CH_3	$COOCH_3$	***a*** $_1$	-501.85161	-501.77127	-16.97	102.34
			a $_2$	-501.85439	-501.76828	-19.16	102.34
			b $_1$	-501.85997	-501.76907	-22.22	106.92
			b $_2$	-501.85737	-501.76800	-20.07	106.92
6	$COOCH_3$	CH_3	***a*** $_1$	-501.85190	-501.76460	-16.11	109.12
			a $_2$	-501.85270	-501.76280	-17.45	109.12
			b $_1$	-501.86300	-501.76333	-25.62	115.08
			b $_2$	-501.86297	-501.76122	-25.64	115.08
7	$COOCH_3$	Cl	***a*** $_1$	-922.13264	-922.04189	-15.87	117.05
			a $_2$	-922.13814	-922.04086	-20.15	117.05
			b $_1$	-922.14619	-922.04192	-27.33	123.02
			b $_2$	-922.14597	-922.03731	-27.19	123.02
8	Cl	$COOCH_3$	***a*** $_1$	-922.13711	-922.04692	-21.03	111.45
			a $_2$	-922.13874	-922.04553	-22.65	111.45
			b $_1$	-922.13923	-922.04830	-23.08	116.96
			b $_2$	-922.13898	-922.04463	-22.96	116.96
9	OCH_3	CH_3	***a*** $_1$	-388.49021	-388.39707	-15.84	127.73
			a $_2$	-388.49279	-388.39598	-17.89	127.73
			b $_1$	-388.50354	-388.39582	-22.90	138.65
			b $_2$	-388.50108	-388.39584	-21.06	138.65
10	CH_3	OCH_3	***a*** $_1$	-388.49162	-388.39714	-17.61	116.54
			a $_2$	-388.49309	-388.39645	-18.75	116.54
			b $_1$	-388.49902	-388.39732	-21.70	116.74
			b $_2$	-388.49729	-388.39747	-20.56	116.74
11	CH_3	CH_3	***a*** $_1$	-313.28428	-313.18917	-19.05	134.11
			a $_2$	-313.28685	-313.18919	-20.92	134.11
			b $_1$	-313.29252	-313.18836	-23.86	134.31
			b $_2$	-313.28999	-313.18795	-23.82	134.31

Table 2. The Activation Barriers, Structural Parameters, Imaginary Frequencies, *para* Delocalization Index of the Transition State and the Transferred Charges in the DA Reactions

Species	$\Delta E_{barrier}$ (kcal mol^{-1})	r_{1-6} (Å)	r_{4-5} (Å)	Frequency (cm^{-1})	PDI	Q_{CT}
1a$_1$-TS	20.59	2.435	2.100	547.8i	0.0904	-0.0538
1a$_2$-TS	21.49	2.209	2.298	558.4i	0.0896	-0.0525
1b$_1$-TS	22.80	2.144	2.399	548.5i	0.0895	-0.0489
1b$_2$-TS	23.02	2.372	2.149	558.3i	0.0906	-0.0452
2a$_1$-TS	20.91	2.394	2.146	534.7i	0.0892	0.0445
2a$_2$-TS	21.37	2.234	2.283	541.7i	0.0893	0.0410
2b$_1$-TS	20.73	2.167	2.375	522.4i	0.0891	0.0354
2b$_2$-TS	20.81	2.323	2.214	527.9i	0.0893	0.0356
3a$_1$-TS	21.13	2.555	2.029	540.6i	0.0865	-0.1001
3a$_2$-TS	22.53	2.257	2.239	566.9i	0.0853	-0.0845
3b$_1$-TS	19.84	2.126	2.477	526.6i	0.0840	-0.0705
3b$_2$-TS	20.81	2.370	2.205	539.6i	0.0867	-0.0510
4a$_1$-TS	21.36	2.635	1.994	515.6i	0.0854	0.1266
4a$_2$-TS	21.35	2.062	2.504	542.6i	0.0856	0.1195
4b$_1$-TS	20.89	1.976	2.682	486.9i	0.0845	0.1240
4b$_2$-TS	21.00	2.634	2.014	499.4i	0.0837	0.1519
5a$_1$-TS	14.22	2.657	2.002	456.9i	0.0841	-0.1448
5a$_2$-TS	16.10	2.099	2.444	485.1i	0.0852	-0.1111
5b$_1$-TS	16.72	2.035	2.595	469.3i	0.0833	-0.1333
5b$_2$-TS	17.39	2.538	2.047	484.4i	0.0864	-0.1160
6a$_1$-TS	19.79	2.473	2.099	498.4i	0.0857	0.0904
6a$_2$-TS	20.92	2.309	2.198	523.7i	0.0871	0.0601
6b$_1$-TS	17.64	2.069	2.553	477.0i	0.0831	0.0832
6b$_2$-TS	18.96	2.190	2.371	501.2i	0.0853	0.0551
7a$_1$-TS	21.64	2.578	2.011	517.1i	0.0877	0.0353
7a$_2$-TS	22.29	2.258	2.237	555.4i	0.0867	0.0020
7b$_1$-TS	18.67	2.021	2.599	495.5i	0.0848	0.0329
7b$_2$-TS	21.57	2.244	2.304	539.5i	0.0860	-0.0085
8a$_1$-TS	16.69	2.614	2.016	472.8i	0.0840	0.0000
8a$_2$-TS	17.56	2.115	2.431	506.7i	0.0851	-0.0676
8b$_1$-TS	15.61	2.042	2.594	467.5i	0.0828	-0.0946
8b$_2$-TS	17.92	2.484	2.092	490.9i	0.0851	-0.0770
9a$_1$-TS	22.44	2.403	2.109	541.1i	0.0876	-0.0073
9a$_2$-TS	23.12	2.281	2.216	550.0i	0.0857	-0.0272
9b$_1$-TS	20.39	2.212	2.369	517.5i	0.0863	-0.0075
9b$_2$-TS	20.38	2.340	2.239	518.3i	0.0866	0.0006
10a$_1$-TS	22.66	2.685	1.942	504.0i	0.0887	0.0927
10a$_2$-TS	23.10	2.073	2.474	545.1i	0.0860	0.0757
10b$_1$-TS	23.67	2.014	2.609	517.2i	0.0869	0.0799
10b$_2$-TS	23.58	2.594	2.00	526.9i	0.0877	0.0952
11a$_1$-TS	21.16	2.423	2.103	536.0i	0.0910	0.0081
11a$_2$-TS	21.14	2.245	2.259	538.7i	0.0902	0.0015
11b$_1$-TS	22.78	2.182	2.354	534.2i	0.0907	0.0039
11b$_2$-TS	23.04	2.39	2.217	536.1i	0.0902	0.0095

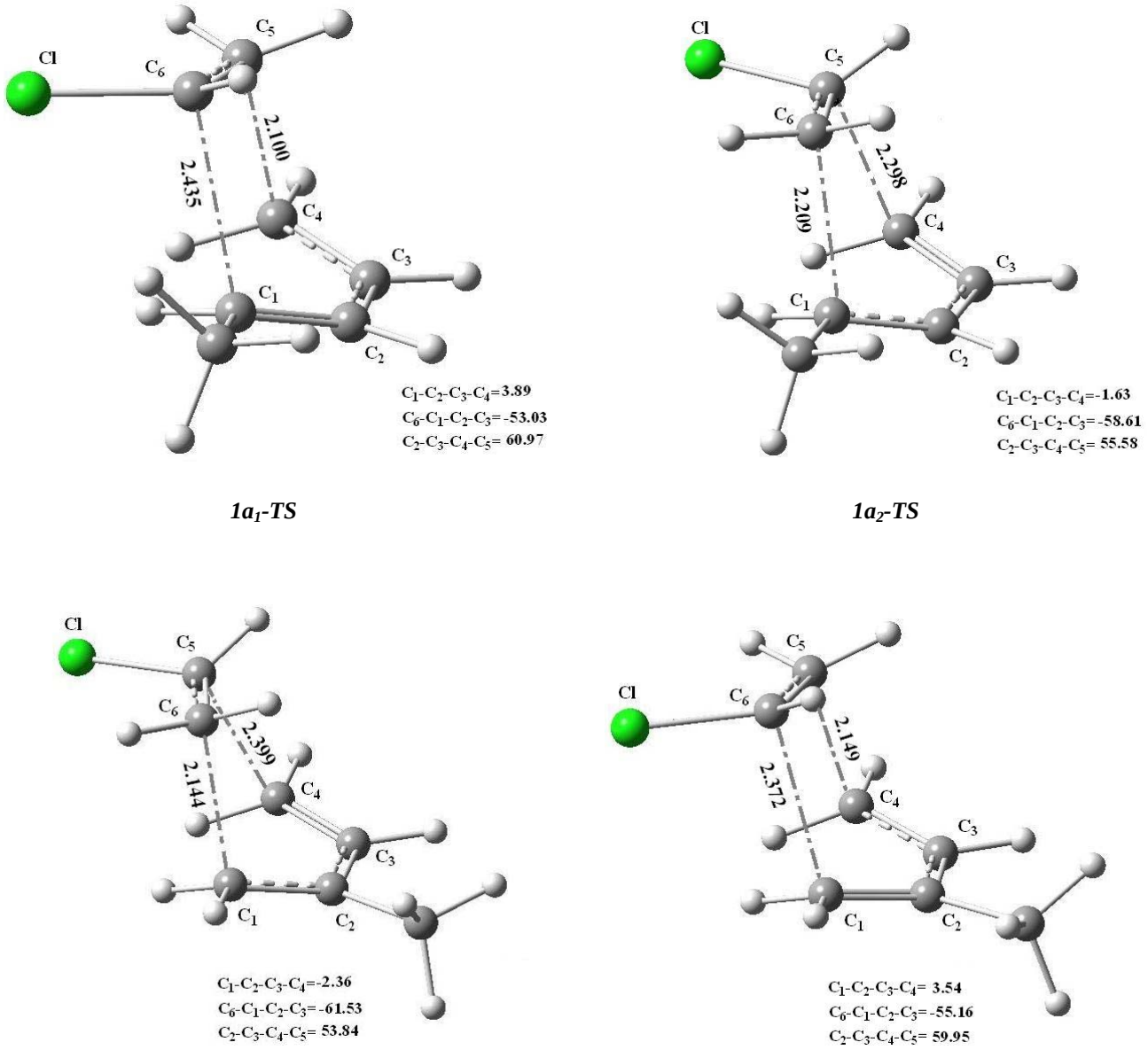

Fig. 1. The optimized structure of transition states of four pathways in reaction 1 (normal type DA reaction). Bond lengths are in angstroms and angles in degree.

CT may be accompanied with a reduction of HLG and a drop of activation barrier.

The reaction mechanism involves the reactants approaching each other on parallel planes with new bonds forming as a result of the overlap of π-electrons clouds. Frontier Molecular Orbital theory (FMO) is used to explain the mechanism. Accordingly, for reaction between an electron-rich and electron-poor reactants, one needs to consider only the nearest pair of frontier orbitals, composed of the HOMO of the former and the LUMO of the latter

compound. Our results show that in the case X and Y are electron-withdrawing substituents such as reaction 8, in which X = Cl and Y = $COOCH_3$, HOMO of the Cl-substituted reactant interacts with LUMO of other components demonstrating more electron-withdrawing power for $COOCH_3$. In neutral case in which X = Y = CH_3, HOMO of the ethylene reacts with LUMO of butadiene, and we have the largest HLG if compared with normal or inverse cases.

In normal DA, the electron-withdrawing substituents such as Cl and $COOCH_3$ reduce the HLG in such a way that is in agreement with the electron-withdrawing power of the substituents, *i.e*. $COOCH_3$ > Cl. The reported HLGs in Table 1 show that in normal and neutral types when butadiene is 1-substituted, HLG is less than the reaction of 2-substituted butadiene, while the situation is reversed for the inverse type DA.

The activation barriers, ($\Delta E_{barrier}$), are calculated as the difference between the energy of the transition state and the sum of the energies of the isolated reactants. The results in Table 2 reveal that in normal and inverse type, for *ortho* and *para* products, the activation barriers are less than their corresponding *meta* adducts. The difference between the activation barrier of pathways $\boldsymbol{a_1}$ and $\boldsymbol{a_2}$ or similarly pathways $\boldsymbol{b_1}$ and $\boldsymbol{b_2}$ is about 1-3 kcal mol^{-1}.

The computed reaction energies in Table 1 suggest that all four pathways are exothermic by 15.84-27.33 kcal mol^{-1}. Among four pathways for each set, the maximum exothermicity is related to pathway $\boldsymbol{b_1}$. It is found that the reaction with the largest exothemicity among the 44 reactions studied here, is the *para* adduct of reaction 7. The thermodynamic pathway achieves a lower energy and hence more stable product. Thus, inspection of the reaction energies establishes the pathway $\boldsymbol{b_1}$ with *para* product is thermodynamically more favorable than the pathway $\boldsymbol{a_1}$ in both normal and inverse types. On the other hand, both pathways $\boldsymbol{a_1}$ and $\boldsymbol{b_1}$ producing the preferred adducts according to *ortho*- and *para*-rules, can be labeled as kinetic pathways. In fact, the regioselectivity is independent of the substituent's electronic effects. The orientation is the same whether the substituent is an electron-donating or an electron-withdrawing group. The potential energy surfaces for the four possible pathways of reaction 1 are illustrated in Fig. 2 as a representative example.

In order to analyze and possibly predict the reactivity behavior of substituted dienes and dienophiles in DA cycloaddition, we have examined the variation of activation barriers with respect to the nature of the substituents. Empirically, quantitative information on the inductive and/or mesomeric nature of substituents is provided respectively by the F and R constants published by Hansch [29]. Boulanger *et al*. found a quasi-linear correlation between the activation barrier and a global electronic effect estimated by F+R for 2-substituted dienes, while a poorer correlation was observed for 1-substituted dienes [30].

Here, we present the correlations between the activation barriers and F+R factor for our selected sets of DA reactions, where both diene and dienophile are mono-substituted. Two different cases are taken into consideration in our analysis. First, we considered dienophile with a specific substituent and changed the substituent on the diene; for instance, when Y is CH_3, X be CH_3, OCH_3, $COOCH_3$ and Cl. Then the correlations between the activation barrier and F+R factor have been checked for four possible pathways in each group and the correlation coefficients (r) are reported in Table 3. In the second case we consider the DA reaction between the diene with fixed substituent and varying substituents on dienophile; for example, where X = CH_3, Y can be CH_3, OCH_3 or $COOCH_3$. The results indicate that there exists better correlation between the activation barriers and the electronic factors in the second case. The discrepancy in the correlation between activation barriers and F+R indicates that sole electronic factors would not be able to explain the barrier height in some cases; rather, the steric factor should also be taken into account.

Aromaticity of the Transition State

The analogy between the π electrons of benzene and the six delocalized electrons in the cyclic transition state of the DA reaction of butadiene and ethylene was recognized by Evans and Warhurst in 1938 [31]. Evans also pointed out that "the greater the mobility of the π-electrons in the transition state, the greater will be the lowering of the activation barrier." In fact, the π-bond alternation in the diene part of the transition state is reduced when the new σ-bonds are formed by disrupting the π-bond of the dienophile resulting in a rehybridization for all carbons. Therefore, six-electron σ,π-mixed cyclic delocalized structure developed in the TS is predicted to be aromatic.

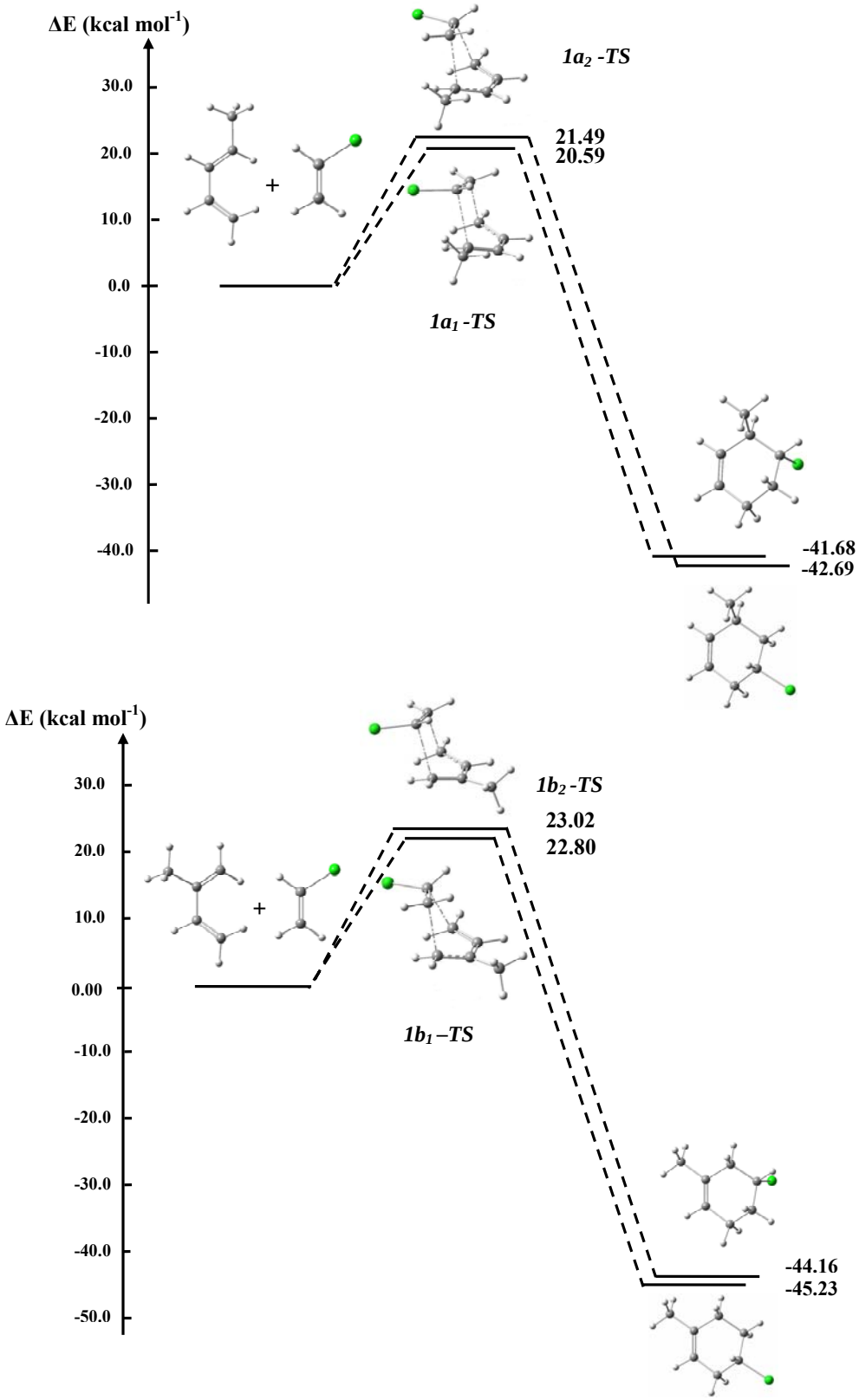

Fig. 2. Schematic energy profiles for four possible pathways of the reaction 1.

Table 3. Correlation Between the Barrier Height and the F+R Factor in Diene and Dienophile Substituted Diels-Alder Reactions

			Correlation coefficients			
X	Y	F+R	a_1	a_2	b_1	b_2
CH_3		-0.34				
OCH_3	CH_3	-0.44	0.423	0.687	0.730	0.637
$COOCH_3$		0.28				
Cl		0.06				
CH_3		0.06				
OCH_3	Cl	-0.04	0.789	0.173	0.624	0. 048
$COOCH_3$		0.68				
	CH_3	-0.34				
CH_3	OCH_3	-0.44	0.872	0.831	0.815	0.805
	$COOCH_3$	0.28				
	Cl	0.06				
	CH_3	0.06				
Cl	OCH_3	-0.04	0.998	0.991	0.994	0.997
	$COOCH_3$	0.68				

In this section the aromaticity of the transition states have been addressed for all the three types of DA reactions. We have employed *para* delocalization index, PDI, to characterize the aromaticity of the transition sates in our 11 sets of DA reactions involving various substituents on both dienes and dienophiles (Table 2). A comparative study of the reported values of PDI for the possible adducts affirms that in normal and neutral type DA, where butadiene is 1-substituted, the transition states of the pathway (a_1) have greater aromaticity character than meta adducts in pathway (a_2). In contrast, in the reaction of 2-substituted butadiene with ethylene the greater aromaticity corresponds to the pathway (b_2) with *meta* adduct. Thus, although it maybe concluded that DA reaction is aromatic in transition state, there is no reason to assume a priori that aromatic character of the TS will lower the activation barrier.

CONCLUSIONS

In the present study, systematic calculations were performed on Diels-Alder reaction to investigate how electronic properties of the diene and dienophile affect the transition states and kinetic or thermodynamic stability of the preferred pathway. In general, we found that the presence of substituents in the diene or dienophile increases the asymmetry of the transition state and decreases the activation barrier. The computed reaction energies and activation barriers for the 4 possible pathways suggest that the pathway b_1 with *para* product is thermodynamically more favorable than the pathway a_1 in both normal and inverse. In fact, the regioselectivity is independent of the substituent's electronic effects.

The correlations between the activation barriers and electronic factors (F+R) of substituents were also investigated for our selected set of DA reactions. The calculated correlation coefficients reveal that the electronic properties of the substituents on both diene and dienophile are not adequate factors for determination of the activation barriers. The role of substituent in the aromaticity of DA reaction is also studied for 11 sets of reaction under consideration. The calculations

suggest that in normal and neutral DA reactions there is a gain in aromatic stabilization of the transition state which reduces slightly the activation barrier of the kinetic pathway $\boldsymbol{a_1}$.

REFERENCES

[1] C.J. Cramer, S.E. Barrows, J. Phys. Org. Chem. 13 (2000) 176.

[2] S. Sakai, J. Phys. Chem. A 104 (2000) 922.

[3] E. Goldstein, B. Beno, K.N. Houk, J. Am. Chem. Soc. 118 (1996) 6036.

[4] A.Z. Bradley, M.G. Kociolek, R.P. Johnson, J. Org. Chem. 65 (2000) 7134.

[5] R.E. Townshend, G. Ramunni, G. Segal, W.J. Hehre, L. Salem, J. Am. Chem. Soc. 98 (1976) 2190.

[6] M.J.S. Dewar, A.B. Pierini, J. Am. Chem. Soc. 106 (1984) 203.

[7] R.A. Firestone, Tetrahedron 52 (1996) 14459.

[8] J.E. Carpenter, C.P. Sosa, J. Mol. Struct. (Theochem) 311 (1994) 325.

[9] K.N. Houk, Y. Li, J.D. Evanseck, Angew. Chem., Int. Ed. Engl. 31 (1992) 682.

[10] L.R. Domingo, M.J. Aurell, P. Perez, R. Contreras, J. Phys. Chem. A 106 (2002) 6871.

[11] M. Manoharan, P. Venuvanalingam, J. Chem. Soc. Perkin Trans. II 9 (1997) 1799.

[12] K.N. Houk, J. Gonzalez, Y. Li, Acc. Chem. Res. 28 (1995) 81.

[13] R.K. Bansal, N. Gupta, S.K. Kumawat, Tetrahedron 62 (2006) 1548.

[14] L.R. Domingo, E. Chamorro, P. Perez, J. Phys. Chem. A. 112 (2008) 4046.

[15] J.W. Storer, L. Raivnondi, K.N. Houk, J. Am. Chem. Soc. 116 (1994) 9675.

[16] M.J.S. Dewar, S. Olivella, J.J.P. Stewart, J. Am. Chem. Soc. 108 (1986) 5771.

[17] S. Sakai, J. Mol. Struct. (Theochem.) 630 (2003) 177.

[18] H.O. Ho, W.K. Li, J. Mol. Struct. (Theochem.) 712 (2004) 49.

[19] R. Robiette, J. Marchand-Brynaert, D. Peeters, J. Org. Chem. 67 (2002) 6823.

[20] H. Jiao, P.V.R. Schleyer, Angew. Chem., Int. Ed. Eng. 32 (1993) 1763.

[21] E. Matito, J. Poater, M. Duran, M. Solà , J. Mol. Struct. (Theochem.) 727 (2005) 165.

[22] C. Gonzalez, H.B. Schlegel, J. Chem. Phys. 90 (1989) 2154.

[23] C. Gonzalez, H.B. Schlegel, J. Phys. Chem. 94 (1990) 5523.

[24] M.J. Frisch, G.W. Trucks, H.B. Schlegel, G.E. Scuseria, M.A. Robb, J.R. Cheeseman, J.A. Montgomery, J.T. Vreven, K.N. Kudin, J.C. Burant, J.M. Millam, S.S. Iyengar, J. Tomasi, V. Barone, B. Mennucci, M. Cossi, G. Scalmani, N. Rega, G.A. Petersson, H. Nakatsuji, M. Hada, M. Ehara, K. Toyota, R. Fukuda, J. Hasegawa, M. Ishida, T. Nakajima, Y. Honda, O. Kitao, H. Nakai, M. Klene, X. Li, J.E. Knox, H.P. Hratchian, J.B. Cross, C. Adamo, J. Jaramillo, R. Gomperts, R.E. Stratmann, O. Yazyev, A.J. Austin, R. Cammi, C. Pomelli, J.W. Ochterski, P.Y. Ayala, K. Morokuma, G.A. Voth, P. Salvador, J.J. Dannenberg, V. G. Zakrzewski, S. Dapprich, A.D. Daniels, M.C. Strain, O. Farkas, D.K. Malick, A.D. Rabuck, K. Raghavachair, J.B. Foresman, J.V. Ortiz, Q. Cui, I. Baboul, R.L. Martin, D.J. Fox, T. Keith, M.A. Al-Laham, C.Y. Peng, A. Nanayakkara, M. Challacombe, P.M.W. Gill, B. Johnson, W. Chen, M. W. Wong, C. Gonzalez, J.A. Pople, Gaussian 03, Revision A.03. Gaussian, Inc., Pittsburgh, PA, 2003.

[25] J. Poater, X. Fradera, M. Duran, M. Solà, Chem. Eur. J. 9 (2003) 400.

[26] R.F.W. Bader, AIM2000 Program, ver 2.0, Hamilton; McMaster University, 2000.

[27] S. Noorizadeh, H. Maihami, J. Mol. Struct. (Theochem.) 763 (2006) 133.

[28] A.E. Reed, L.A. Curtiss, F. Weinhold, Chem. Rev. 88 (1988) 899.

[29] a) C. Hansch, A. Leo, R.W. Taft, Chem. Rev. 91 (1991) 165; b) C.G. Swain, E.C. Lupton Jr., J. Am. Chem. Soc. 90 (1968) 4328.

[30] M. Boulanger, T. Leyssens, R. Robiette, D. Peeters, J. Mol. Struct. (Theochem.) 731 (2005) 101.

[31] M.G. Evans, E. Warhurst, Trans. Faraday Soc. 34 (1938) 614.